

# Generative Adversarial Symmetry Discovery

Jianke Yang<sup>1</sup> Robin Walters<sup>\*2</sup> Nima Dehmamy<sup>\*3</sup> Rose Yu<sup>1</sup>

## Abstract

Despite the success of equivariant neural networks in scientific applications, they require knowing the symmetry group a priori. However, it may be difficult to know the right symmetry to use as an inductive bias in practice and enforcing the wrong symmetry could hurt the performance. In this paper, we propose a framework, LieGAN, to *automatically discover equivariances* from a dataset using a paradigm akin to generative adversarial training. Specifically, a generator learns a group of transformations applied to the data, which preserves the original distribution and fools the discriminator. LieGAN represents symmetry as interpretable Lie algebra basis and can discover various symmetries such as rotation group  $SO(n)$  and restricted Lorentz group  $SO(1, 3)^+$  in trajectory prediction and top quark tagging tasks. The learned symmetry can also be readily used in several existing equivariant neural networks to improve accuracy and generalization in prediction.

## 1. Introduction

Equivariance has always been an important inductive bias in deep learning. For example, convolutional neural networks exploit translational symmetry in images, and graph neural networks utilize permutation symmetry in graph-structured data (Kipf & Welling, 2016). Symmetry-aware equivariant networks have led to significant improvement in generalization, sample efficiency and scientific validity (Zaheer et al., 2017; Weiler & Cesa, 2019; Cohen et al., 2019a; Wang et al., 2021). Interest has surged in both theoretical analysis and practical techniques for building general group equivariant neural networks (Kondor & Trivedi, 2018; Cohen et al., 2019b; Bekkers, 2019; Finzi et al., 2021).

However, a key limitation of equivariant neural networks is that they require explicit knowledge of the task symmetry before a model can be constructed. In practice, it is sometimes difficult to identify the true symmetries of the

task, and constraining the model by the exact mathematical symmetry might not be optimal in real-world datasets (Wang et al., 2022). These challenges call for approaches that enable deep learning methods to automatically discover the underlying symmetry of the tasks.

Neural networks that discover unknown symmetry may play the role of AI scientists, not only by making data-driven predictions, but also by identifying and describing physical systems through their symmetries and generating new scientific insights through the close relationship between symmetry, conservation laws and underlying governing equations (Alet et al., 2021). Most existing works in symmetry discovery can only address a small fraction of potential symmetry types, such as finite groups (Zhou et al., 2020), subsets of a given group (Benton et al., 2020) or individual group elements (Desai et al., 2021). L-conv (Dehmamy et al., 2021) can discover continuous symmetries without discretization of the groups, but is limited in computational efficiency. A more general framework is needed for the discovery of various real-world symmetries.

In this work, we present a novel framework for discovering continuous symmetry from data using generative adversarial training (Goodfellow et al., 2014). Our method trains a symmetry generator that transforms the training data and outputs a similar distribution to the original dataset, which suggests equivariance or invariance to the learned transformations. Making use of the theory of Lie groups and Lie algebras, our method, *LieGAN*, is able to discover continuous symmetries as matrix groups. Moreover, through different parameterization strategies, it can also deal with other types of symmetries, such as discrete group transformation, as well as the subset of a group.

Our main contributions can be summarized as follows:

1. We propose LieGAN, a method for discovering symmetries in datasets, capable of learning general linear symmetries, including the rotation group  $SO(n)$  and restricted Lorentz group  $SO(1, 3)^+$ .
2. LieGAN is interpretable, directly yielding an orthogonal Lie algebra basis as a discovery result.
3. We show that the Lie algebra learned by LieGAN leads to excellent performance in downstream tasks such as

<sup>\*</sup>Equal contribution <sup>1</sup>University of California San Diego

<sup>2</sup>Northeastern University <sup>3</sup>IBM Research. Correspondence to: Rose Yu <roseyu@ucsd.edu>.

$N$ -body dynamics and top quark tagging.

4. We propose LieGNN, a modified EGNN (Satorras et al., 2021) which incorporates symmetries learned by LieGAN, with performance close to equivariant models using ground truth symmetries.

## 2. Related Work

**Equivariant Neural Networks.** Many works have addressed the problems of designing neural network modules that are equivariant to specific transformations, such as permutation in sets (Zaheer et al., 2017), local gauge transformations (Cohen et al., 2019a), scaling (Worrall & Welling, 2019), rotation on spheres (Cohen et al., 2018) and general  $E(2)$  transformations on Euclidean plane (Weiler & Cesa, 2019). Another branch of works focus on developing theoretical guidelines and practical methods for building general group equivariant neural networks (Cohen & Welling, 2016; Kondor & Trivedi, 2018; Cohen et al., 2019b; Finzi et al., 2020; 2021). These methods rely on explicit a priori knowledge of the task symmetry and cannot be used when such information is unavailable. Unlike these approaches, we are interested in discovering knowledge of the symmetry itself. The learned symmetry can then be used to select or design an equivariant neural network to make predictions.

**Generative Adversarial Training.** The original generative adversarial network (GAN) (Goodfellow et al., 2014) uses a generator to transform random noise into target distribution. Many variants of GAN have been proposed to address different tasks other than unrestricted generation. For example, CycleGAN (Zhu et al., 2017) learns a generator that maps the input image to another domain. DAGAN (Antoniou et al., 2017) also takes data points from a source domain and generalizes them to a broader domain with a generator to perform data augmentation, which is related to our task, as the augmenting process can be regarded as a set of transformations to which the data is invariant. These works use samples from the original distribution instead of random noise as generator input and perform domain transfer or generalization with a generator. Our work proposes another usage of such design. The generator in our model produces transformations which are applied to data samples, and discovers the underlying symmetry by learning the correct set of transformations.

**Symmetry Discovery.** Most existing symmetry discovery methods (Benton et al., 2020; Zhou et al., 2020; Dehmamy et al., 2021) build on a supervised setting to extract symmetry from data while learning another task. These works are generally limited in terms of their search space for symmetry groups. MSR (Zhou et al., 2020) reparameterizes network weights into task weights and a symmetry matrix

and meta-learns the symmetry matrix to provide information about task symmetry. However, it can only be applied to finite groups and scales linearly in space complexity with the size of the group, which eliminates the possibility of applying this algorithm to infinite continuous groups. Also, it remains to be seen whether this approach can learn interpretable symmetry matrices in tasks with more complex symmetries than translation. Augerino (Benton et al., 2020) addresses a different but relevant scenario: learning the extent of symmetry within a given group. Partial G-CNN (Romero & Lohit, 2021) also learns group subsets via distributions on group to describe the symmetry at different levels in the model. These approaches can only be applied to cases where the symmetry group has been specified, like rotation for 2D images. This work aims to address all of these problems within a unified framework.

L-conv (Dehmamy et al., 2021) develops a Lie algebra convolutional network that can model any group equivariant functions. However, it performs first order approximation for matrix exponential and uses recursive layers to push the kernel away from the identity, which may become too expensive in practice. Moreover, the experiments are limited to image datasets.

Another existing work (Desai et al., 2021) also proposes to discover symmetries of the dataset distribution with a GAN. A major limitation of their algorithm is that the model can only learn one group element in a single round of training and has to rely on other techniques such as subgroup regularization or group composition to identify the group. Also, they are addressing a different definition of symmetry from our case.

Comparison between LieGAN and other works on symmetry discovery can be found in Table 1. To the best of our knowledge, our approach is the *first* to address the discovery of such a variety of symmetries including discrete group, continuous group, and subset of given or unknown group.

Table 1. Comparison of different models’ capability of discovering different kinds of symmetries

SYMMETRY	MSR	AUGERINO	LIEGAN
DISCRETE	✓	✗	✓
CONTINUOUS	✗	✗	✓
GIVEN GROUP SUBSET	✗	✓	✓
UNKNOWN GROUP SUBSET	✗	✗	✓

## 3. Background

Before presenting our methodology, we provide some preliminary concepts that appear frequently in our work. We assume basic knowledge about group theory.

**Lie group.** A Lie group is a group that is also a differentiable manifold. It can be used to describe continuous transformations. For example, all 2D rotations form a Lie group  $SO(2)$ , where rotation with angle  $\theta$  can be represented by  $R = \begin{bmatrix} \cos \theta & -\sin \theta \\ \sin \theta & \cos \theta \end{bmatrix}$ . Also, all Euclidean transformations including reflection, rotation and translation form the Lie group of  $E(n)$ . Each Lie group is associated with a Lie algebra, which is its tangent vector space at identity:  $\mathfrak{g} = T_{\text{Id}}G$ . The basis of the Lie algebra  $L_i \in \mathfrak{g}$  are called (infinitesimal) generators of the Lie group. Group elements that are infinitesimally close to identity can be written in terms of these generators:  $g = \text{Id} + \sum_i \epsilon_i L_i$ .

We can use an exponential map  $\exp : \mathfrak{g} \rightarrow G$  to map Lie algebra elements to Lie group elements. For matrix groups, matrix exponential is such a map. For a connected Lie group  $G$ , its elements can be written as  $g = \exp(\sum_i w_i L_i)$ .

**Group representation.** We are interested in how group elements transform the data. We assume the input space is  $\mathcal{X} = \mathbb{R}^n$ . A group element  $g \in G$  can act linearly on  $x \in \mathcal{X}$  via  $\rho_{\mathcal{X}}(g)$ , where  $\rho_{\mathcal{X}} : G \rightarrow GL(n)$  is a group representation.  $\rho_{\mathcal{X}}$  maps each group element  $g$  to a nonsingular matrix  $\rho_{\mathcal{X}}(g) \in \mathbb{R}^{n \times n}$  that transforms the input vector.

A group representation  $\rho : G \rightarrow GL(n)$  induces a representation for the Lie algebra  $\mathfrak{g} = T_{\text{Id}}G$  denoted as  $d\rho : \mathfrak{g} \rightarrow \mathfrak{gl}(n)$ , which relate to the representation of its Lie group by  $\exp(d\rho(L)) = \rho(\exp(L))$ .

## 4. Symmetry Discovery

We aim to automatically discover symmetry from data. By symmetry in a dataset, we refer to the *equivariance* property of a function. Formally, let  $\mathcal{D} = \{(x_i, y_i)\}_{i=1}^N$  be a dataset with distribution  $x_i, y_i \sim p_d(x, y)$ , input space  $\mathcal{X} = \mathbb{R}^n$ , output space  $\mathcal{Y} = \mathbb{R}^m$  and an unknown function  $f : \mathcal{X} \rightarrow \mathcal{Y}$ . We have:

**Definition 1 (Equivariance).** Suppose a group  $G$  acts on  $\mathcal{X}$  and  $\mathcal{Y}$  via representations  $\rho_{\mathcal{X}} : G \rightarrow GL(n)$  and  $\rho_{\mathcal{Y}} : G \rightarrow GL(m)$ . Then, a function  $f : \mathcal{X} \rightarrow \mathcal{Y}$  is *equivariant* if  $\forall g \in G, (x, y) \in \mathcal{D}, \rho_{\mathcal{Y}}(g)y = f(\rho_{\mathcal{X}}(g)x)$ . We omit  $\rho_{\mathcal{X}}$  and  $\rho_{\mathcal{Y}}$  when clear and write  $gy = f(gx)$ .

We also address invariance in this work, which is a special case of equivariance when  $\rho_{\mathcal{Y}}(g) = \text{Id}$ . Next, we describe the formulation to relate symmetry discovery with generative adversarial training (Goodfellow et al., 2014).

### 4.1. Generative Adversarial Symmetry Discovery

By Definition 1, if a group element acts on the input, the output of an equivariant function is also transformed correspondingly by the representation of the same element. From

another perspective, if all the data samples are transformed in this way, the group transformed data distribution should remain similar to the original dataset distribution.

At a high level, we want to design a generator that can efficiently produce transformed input and a discriminator that can not distinguish real samples from the dataset and the outputs from the generator. Through adversarial training, the generator tries to fool the discriminator by learning a group of transformations that minimizes the divergence between the transformed and the original distributions. This group of transformations defines the symmetry of interest.

We are interested in how the group  $G$  acts on data through its two representations  $\rho_{\mathcal{X}}$  and  $\rho_{\mathcal{Y}}$ . We learn  $G$  as a subgroup of  $GL(k)$  for some  $k$  chosen based on the task. The representations  $\rho_{\mathcal{X}} : GL(k) \rightarrow GL(n)$  and  $\rho_{\mathcal{Y}} : GL(k) \rightarrow GL(m)$  are also chosen and fixed based on the task. The GAN generator  $\Phi$  samples an element from a distribution  $\mu$  defined on  $GL(k)$  and then applies it to  $x$  and  $y$ :

$$\Phi(x, y) = (\rho_{\mathcal{X}}(g)x, \rho_{\mathcal{Y}}(g)y) \quad (1)$$

For an invariant task, for example, we set  $k = n$  and  $\rho_{\mathcal{X}} = \text{Id}$  the standard representation and  $\rho_{\mathcal{Y}} = 1$  the trivial representation. For a time series prediction task predicting a system state based on  $t$  previous states, we set  $k = m$  and  $n = tm$  and  $\rho_{\mathcal{X}} = \text{Id}^{\oplus t}$  and  $\rho_{\mathcal{Y}} = \text{Id}$ .

Under this formulation, the generator should learn a subgroup of the transformations to which  $f : \mathcal{X} \rightarrow \mathcal{Y}$  is equivariant. That is, it should generate a distribution close to the original data distribution. Similar to the setting in GAN, we optimize the following minimax objective:

$$\begin{aligned} & \min_{\Phi} \max_D L(\Phi, D) \\ &= \mathbb{E}_{x, y \sim p_d, g \sim \mu} [\log D(x, y) + \log(1 - D(\Phi(x, y)))] \\ &= \mathbb{E}_{x, y \sim p_d} [\log D(x, y)] + \mathbb{E}_{x, y \sim p_g} [\log(1 - D(x, y))] \end{aligned} \quad (2)$$

where  $D$  is a standard GAN discriminator that outputs a real value as the probability that  $(x, y)$  is a real sample,  $p_d$  is the density of the original data distribution and  $p_g$  is the generator-transformed distribution given according to change-of-variable formula by

$$p_g(x, y) = \int_g \mu(g) p_d(g^{-1}x, g^{-1}y) / (|\rho_{\mathcal{X}}(g)| |\rho_{\mathcal{Y}}(g)|) dg \quad (3)$$

Under the ideal discriminator, the generator of GAN minimizes the JS divergence between two distributions (Nowozin et al., 2016). In our setting, we prove that our generator can achieve zero divergences with the correct symmetry group under certain circumstances.

**Theorem 1.** *The generator can achieve zero JS divergence by learning a maximal subgroup  $G^* \subset GL(n)$  with re-*

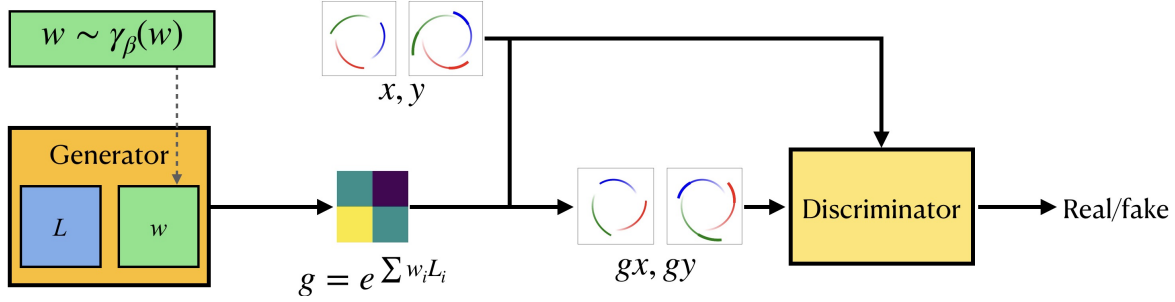


Figure 1. Structure of the proposed LieGAN model. The transformation generator learns a continuous Lie group acting on the data that preserves the original joint distribution. For example, this figure shows a task of predicting future 3-body movement based on past observations, where the generator could learn rotation symmetry.

spect to which  $y = f(x)$  is equivariant if  $p_d(x)$  is distributed proportionally to the volume of inverse group element transformation along each orbit of  $G^*$ -action on  $\mathcal{X}$ , that is,  $p_d(gx_0) \propto |\rho_{\mathcal{X}}(g^{-1})| |\rho_{\mathcal{Y}}(g^{-1})|$ .

The hypothesis of Theorem 1 is equivalent to saying that  $p_d(x)$  is uniform along each group action orbit when the transformation is volume preserving, as in the case of rotation. However, as this is often not satisfied in practice, there is no guarantee that the generator can achieve zero divergences with nonidentical transformations. Nevertheless, as formalized in the following theorem, the generator can learn a nontrivial symmetry under some weak assumptions.

**Theorem 2.** *Under assumptions 1,2 and 3, the GAN loss function under the ideal discriminator  $L(\Phi, D^*)$  is lower with a generator that learns a subspace of the true Lie algebra  $\mathfrak{g}^*$  than a generator with an orthogonal Lie algebra to  $\mathfrak{g}^*$ . That is, if  $\mathfrak{g}_1 \cap \mathfrak{g}^* \neq \{0\}$ ,  $\mathfrak{g}_2 \cap \mathfrak{g}^* = \{0\}$ , then  $L(\mathfrak{g}_1, D^*) < L(\mathfrak{g}_2, D^*) = 0$ .*

Theorem 2 ensures that a partially correct symmetry results in lower loss function value than an incorrect symmetry. In other words, optimizing (2) leads to symmetry discovery.

The related assumptions and proofs for Theorem 1 and 2 are deferred to Appendix A.1.

#### 4.2. Parameterizing Distributions Over Lie Group

We use the theory of Lie groups to model continuous sets of transformations. To parameterize a distribution on a Lie group with  $c$  dimensions and  $k$  representation dimensions, our model learns Lie algebra generators  $\{L_i \in \mathbb{R}^{k \times k}\}_{i=1}^c$  and samples the coefficients  $w_i \in \mathbb{R}$  for their linear combination from either a fixed or a learnable distribution. The Lie algebra element is then mapped to a Lie group element using matrix exponential. (Falorsi et al., 2019)

$$w \sim \gamma_\beta(w), \quad g = \exp \left[ \sum_i w_i L_i \right] \quad (4)$$

The coefficient distribution  $\gamma_\beta$  can be either fixed or updated, depending on our focus of discovery. If we have little information on the group, then by learning the  $L_i$  and leaving the coefficient distribution fixed, our model can still express distributions over many different groups. On the other hand, we may want to find a subgroup or a subset of some known group. For example, the symmetry may be some discrete subgroup of  $SO(2)$  for some tasks. In this case, we fix  $L$  as the rotation generator and learn  $\gamma_\beta$ , revealing peaks at certain values. Learning  $\gamma_\beta$  is also useful when the task is not equivariant to the full group, but displays invariance for a subset of transformations, for example, the case of MNIST image classification where rotating by  $\pi$  will obscure the boundary between “6” and “9” (Benton et al., 2020). Generally, allowing for  $\beta$  to be learnable gives the model more freedom to discover various symmetries.

The coefficient distribution  $\gamma_\beta$  may be parameterized in different ways. A normal distribution centered at the origin is a natural choice, since it assigns the same probability density for a group element and its inverse, and the variance can either be fixed or learned through the reparameterization trick (Kingma & Welling, 2013). However, a multimodal distribution like a Gaussian mixture model may be better at capturing discrete subgroups.

However, we note that a limitation of using the Lie algebra to parameterize transformations is that it can only capture a single connected component of the Lie group. Some groups such as  $E(n)$  do not have a surjective exponential map and their group elements must be described by introducing additional discrete generators:  $g = \exp[\sum_i t_i L_i] \prod_j h_j$ .

#### 4.3. Regularization Against Trivial Solutions

In our optimization problem (2), the generator can learn a trivial symmetry of identical transformation, which makes the generated distribution exactly the same as the original distribution. We alleviate this issue by penalizing the similarity between the input and output of the generator. Let  $R$  be similarity function on  $\mathcal{X} \times \mathcal{Y}$ . In practice we use cosine

similarity. The regularizer is then defined

$$l_{\text{reg}}(x, y) = R(\Phi(x, y), (x, y)). \quad (5)$$

Another issue arises when dealing with multi-dimensional Lie groups. The model is encouraged to search through different directions in the manifold of general linear group with multiple channels, i.e.  $L_i$ 's. In practice, however, we find that they tend to learn similar elements. To address this problem, we introduce another regularization against the channel-wise similarity, denoted as

$$l_{\text{chreg}}(\Phi) = \sum_{1 \leq i < j \leq c} R_{\text{ch}}(L_i, L_j) \quad (6)$$

where  $c$  is the number of channels in generator and  $R_{\text{ch}}$  is the cosine similarity for  $L_i$  weights. We also consider setting  $R_{\text{ch}}$  to be the Killing form (Knapp & Knapp, 1996), a metric defined on the Lie algebra. In that case, minimizing  $l_{\text{chreg}}$  corresponds to discovering an orthogonal basis for the Lie algebra. In practice, we find that cosine similarity works best.

Combining these regularizers with (2), we optimize the following objective:

$$L_{\text{reg}}(\Phi, D) = \mathbb{E}_{(x, y), g} [\log D(x, y) + \log(1 - D(\Phi(x, y)))] + \lambda \cdot l_{\text{reg}}(x, y) + \eta \cdot l_{\text{chreg}}(\Phi) \quad (7)$$

#### 4.4. Model Architecture

LieGAN consists of two components, the generator and the discriminator. The generator simply samples a Lie group element to transform the input data and does not have any deep neural network. The discriminator can be any network architecture that fits the input. In practice, we use Multi-layer Perceptron (MLP) as a discriminator unless otherwise stated. We find that the generator loss is usually higher than the discriminator loss during training, which suggests that the generator's task of finding the correct set of symmetry transformations is harder. Therefore, a simple discriminator architecture is sufficient.

### 5. Using the Discovered Symmetry

The discovered symmetry can be used as an inductive bias to aid prediction. For instance, Augerino (Benton et al., 2020) develops an end-to-end pipeline that simultaneously discovers invariance and trains an invariant model. For our method, there are multiple ways of utilizing the learned Lie algebra representation in downstream prediction tasks.

#### 5.1. Data Augmentation

A natural idea would be augmenting the training data with the transformation generator in LieGAN, which should lead

to better generalization and robustness just as any other data augmentation approaches (Dao et al., 2019). To perform data augmentation in the equivariance scenario, we transform the input with group element  $g$  and transform the model output with  $g^{-1}$  to obtain the final prediction

$$\hat{y} = g^{-1} f_{\text{model}}(gx). \quad (8)$$

#### 5.2. Equivariant Model

The discovered symmetry from LieGAN can also be easily incorporated into existing equivariant models due to its explicit representation of the Lie algebra. This procedure is specific to different equivariant model architectures. We provide two examples of incorporating the learned symmetry into EMLP (Finzi et al., 2021) and EGNN (Satorras et al., 2021), which are also used in experiments.

**EMLP.** Finzi et al. (2021) provide a simple interface for building equivariant MLPs for arbitrary matrix groups. We can directly use the discovered Lie algebra basis as input to the method and find an MLP equivariant to the corresponding connected Lie group, with only a minor modification to the model. The original EMLP constructs a constraint matrix according to the specified group, and projects network weights to its null space. This does not work well with the symmetry discovered by LieGAN, because it inevitably has some numerical error that results in a higher rank constraint matrix and thus lower rank weight matrix. In practice, we raise the singular value threshold to get an approximate equivariant subspace with more dimensions. Implementation details can be found in Appendix B.1.

**EGNN.** Satorras et al. (2021) encode  $E(n)$  equivariance in a GNN by computing invariant edge features using the Euclidean metric. Similarly, Gong et al. (2022) develop a Lorentz invariant GNN for jet tagging by computing invariant edge features using the Minkowski metric. Both methods may be summarized as:

$$m_{ij} = \phi_e(h_i, h_j, \|x_i - x_j\|_J^2, \langle x_i, x_j \rangle_J) \\ \text{where } \|u\|_J = \sqrt{u^T J u}, \quad \langle u, v \rangle_J = u^T J v \quad (9)$$

where  $h_i$  and  $h_j$  are scalar node features,  $\|\cdot\|_J^2$  and  $\langle \cdot \rangle_J^2$  are norms and inner products computed with metric tensor  $J$  and  $\phi_e$  is a neural network. The tensor  $J$  can be varied to enforce different symmetries, such as  $\text{diag}(1, -1, -1, -1)$  for  $O(1, 3)$  and  $\text{Id}_n$  for  $E(n)$ . Under this formulation, the input features for  $\phi_e$  are group invariant scalars, which leads to equivariance of the entire architecture.

However, the selection of metric tensor  $J$  relies on knowledge of the specific symmetry group, and the application of such equivariant models is restricted if no a priori knowledge about the symmetry is readily available. We will show

that the discovered symmetry from LieGAN can replace the requirement of theoretical knowledge through a simple procedure. First, we derive an equivalent relation between an arbitrary Lie group symmetry and its invariant metric tensor (see Appendix A.3 for proof).

**Proposition 1.** *Given a Lie algebra basis  $\{L_i \in \mathbb{R}^{k \times k}\}_{i=1}^c$ ,  $\eta(u, v) = u^T J v$  ( $u, v \in \mathbb{R}^k, J \in \mathbb{R}^{k \times k}$ ) is invariant to infinitesimal transformations in the Lie group  $G$  generated by  $\{L_i\}_{i=1}^c$  if and only if  $L_i^T J + J L_i = 0$  for  $i = 1, 2, \dots, c$ .*

This suggests that if we have the discovered a Lie algebra basis  $\{L_i\}_{i=1}^c$ , we can obtain the invariant metric tensor  $J$  for the corresponding Lie group easily by solving a linear equation. However, directly solving this system gives a zero solution for  $J$ . Also, as the basis discovered by LieGAN inevitably has some numerical error, there might not be a nonzero solution. Taking these into consideration, we add a regularization term and optimize the following objective to get an approximation of ideal metric tensor

$$\arg \min_J \sum_{i=1}^c \|L_i^T J + J L_i\|^2 - a \cdot \|J\|^2 \quad (10)$$

with  $a > 0$ . The choice of regularization coefficient  $a$  and the type of matrix norm can be largely arbitrary. A small push from zero is sufficient to get a reasonable metric  $J$ . With this approach, we can construct equivariant GNN for any discovered Lie group, which we refer to as LieGNN.

## 6. Experiments

We experiment on several tasks to demonstrate the capability of LieGAN. Specifically, we aim to validate (1) whether LieGAN can discover different types of symmetries mentioned in Table 1; (2) whether the discovered symmetry, combined with existing models, can boost prediction performance.

### 6.1. Baselines

Direct comparison with other symmetry discovery methods is not always possible, since these works deal with different settings for discovery (see Table 1). MSR (Zhou et al., 2020) uses a largely different discovery scheme from ours and can only learn finite symmetry groups, so it is not included in the experiments. SymmetryGAN (Desai et al., 2021) only learns an individual group element, which differs from our definition of symmetry discovery. We only include it in the first experiment to explain the difference. We mainly compare our method with Augerino (Benton et al., 2020), which also learns with Lie algebra representation. Augerino was originally developed for discovering a subset of a given group rather than an unknown symmetry group. We adapted Augerino from parameterizing the distribution over the given group to the distribution over the

entire general linear group search space. Specifically, in the original Augerino forward function

$$f_{\text{aug-eq}}(x) = \mathbb{E}_{g \sim \mu} g^{-1} f(gx), \quad (11)$$

we parameterize the distribution  $\mu$  as in Equation (4). This provides ground for comparison between our method and theirs. To differentiate between this modified version with the original Augerino, we denote this approach as Augerino+ in the following discussion.

Also, we incorporate the symmetry learned by the discovery algorithms into compatible models such as EMLP (Finzi et al., 2021) and LorentzNet (Gong et al., 2022). It should be noted that these prediction models are not directly comparable with our method since they use known symmetry whereas we focus on symmetry discovery. We combine them with LieGAN to verify whether our learned symmetry representation leads to comparable prediction accuracy with the exact symmetry in theory.

### 6.2. N-Body Trajectory

We test our model as well as the baselines, Augerino and SymmetryGAN, on the simulated n-body trajectory dataset from Hamiltonian NN (Greydanus et al., 2019). It consists of the interdependent movements of multiple masses. We use a setting where two bodies with identical masses rotate around one another in nearly circular orbits. The task is to predict future movements based on the past series, which is rotational equivariant. The input and output feature for each timestep has  $4n$  dimensions, consisting of the positions and momentums of all bodies:  $[q_{1x}, q_{1y}, p_{1x}, p_{1y}, \dots, q_{nx}, q_{ny}, p_{nx}, p_{ny}]$ .

We search for symmetries acting on the position and momentum of each mass separately, which induces a parameterization of  $2 \times 2$  block diagonal matrix for the generator.

As is shown in Figure 2, LieGAN can discover a symmetry that is nearly identical to ground truth, with a cosine correlation of 0.9998. We should note that the scale of the generator should not be taken into consideration when we compare different representations, because they are basis in the Lie algebra and are scale irrelevant. In contrast, Augerino+ only achieves a cosine similarity of 0.4880 with ground truth, which suggests that Augerino cannot be readily applied to discovering unknown groups.

On the other hand, SymmetryGAN (Desai et al., 2021) produces a very similar visualization to ground truth symmetry. However, this result has a completely different interpretation. Instead of a Lie algebra generator that generates the entire group, SymmetryGAN is learning only one element of the group. In this case, it learns a rotation by  $\frac{\pi}{2}$ , which coincides with the Lie algebra generator.

In addition, we expand the symmetry search space of Lie-

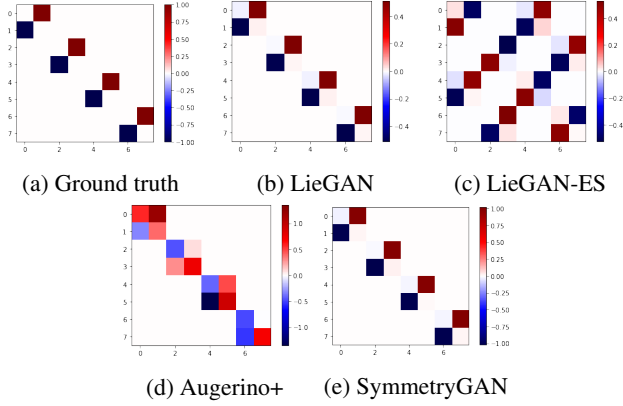


Figure 2. Comparison between different methods on 2-body trajectory dataset. LieGAN discovers the correct rotation symmetry with both the original parameterization and the alternative parameterization with expanded search space (LieGAN-ES), whereas Augerino+ fails. SymmetryGAN only discovers one element in the group.

GAN to enable interactions between the position or momentum of different bodies. The result is shown in Figure 2c. Given that the origin is located at the center of mass and that the two bodies have the same mass, this can be viewed as another possible representation of the same rotation symmetry. Details of derivation for this result are included in Appendix A.2.

Table 2. Test MSE loss of 2-body trajectory prediction. LieGAN and LieGAN-ES correspond to different parameterizations of our model as is shown in Figure 2. Symmetries from different discovery models and ground truth are inserted into EMLP or used to perform data augmentation. HNN is also included for comparison between equivariant models and model with other types of inductive bias.

Model	EMLP	Data Aug.
LieGAN	6.43e-5	3.79e-5
LieGAN-ES	2.41e-4	6.17e-5
Augerino+	9.41e-4	1.47e0
SymmetryGAN	-	6.79e-4
Ground truth	<b>9.45e-6</b>	<b>1.39e-5</b>
HNN	3.63e-4	
MLP	8.49e-2	

Besides the interpretation of the learned symmetry, we can also inject it into equivariant MLP or use it to augment the training data. For prediction, the train and test datasets are constructed to have different distributions so that knowledge of symmetry would be useful for generalization. The results are shown in Table 2. All experiments use the same configuration for MLP except for the introduced equivariance or

data augmentation procedure. For Equivariant MLP, the two parameterizations of LieGAN outperform other symmetry discovery methods, approaching the performance of ground truth symmetry. MLP with no equivariance constraint can achieve lower training loss, but has trouble generalizing to a test set with the shifted distribution. For data augmentation, LieGAN can also achieve comparable accuracy to ground truth symmetry. SymmetryGAN only transforms the data by a fixed transformation, and its performance lies between continuous augmentation and no augmentation.

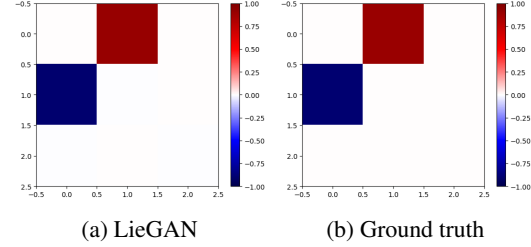


Figure 3. Result on the synthetic discrete rotation invariant task.

### 6.3. Synthetic Regression

Next, we apply LieGAN to a synthetic regression problem given by  $f(x, y, z) = z / (1 + \arctan \frac{y}{x} \bmod \frac{2\pi}{k})$ . This function is invariant to rotations of a multiple of  $2\pi/k$  in the  $xy$  plane, which form a discrete cyclic subgroup of  $SO(2)$  with a size of  $k$ . The goal is to demonstrate that our model can capture the symmetries of not only continuous Lie groups but also their discrete subgroups.

In this task, we fix the coefficient distribution to a uniform distribution on an integer grid of  $[-10, 10]$  to capture discrete symmetry. Figure 3 shows an example of LieGAN discovery in a dataset with  $C_7$  rotation symmetry. The discovered symmetry is almost identical to ground truth, with an MAE of 0.003. Unlike the previous case of continuous rotation, the scale of the basis matters because LieGAN is modeling a set of discrete rotation symmetries with fixed angles. LieGAN discovers not only the rotation group but also the correct scale of transformations, which demonstrates its ability to learn a subgroup of an unknown group, which is yet another generalization from discovering the continuous symmetry of an entire Lie group.

### 6.4. Top tagging

We are also interested in finding symmetry groups with more complicated structures. For example, Lorentz group is an important set of transformations in many physics problems. It is a 6-dimensional Lie group with 4 connected components. While our method cannot be readily generalized to the problem of finding discrete generators, we can test whether it is capable of extracting the identity component of the Lorentz group,  $SO(1, 3)^+$ . We use Top Quark Tagging



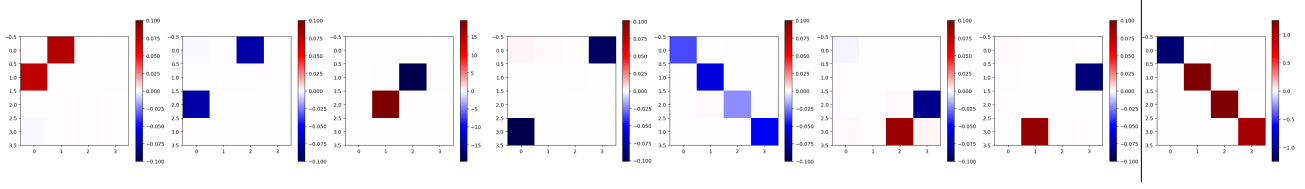


Figure 4. Left: LieGAN discovers an approximate  $SO(1, 3)^+$  symmetry in top tagging dataset, where channels 0, 1, 3 indicate boost along x-, y- and z-axis and channels 2, 5, 6 correspond to  $SO(3)$  rotation. Right: Computed invariant metric of the discovered symmetry by solving Equation (10).

Table 3. Test accuracy and AUROC on top tagging. Our proposed model, LieGNN, reaches the performance with LorentzNet which explicitly encodes Lorentz symmetry. The result of non-equivariant GNN (LorentzNet (w/o) and EGNN is from Gong et al. (2022).

Model	Accuracy	AUROC
LorentzNet	<b>0.940</b>	<b>0.9857</b>
LieGNN	0.938	0.9848
LorentzNet (w/o)	0.934	0.9832
EGNN	0.922	0.9760

Reference Dataset (Kasieczka et al., 2019) for discovering Lorentz symmetry, where the task is to classify between top quark jets and lighter quarks. There are 2M observations in total, each consisting the four-momentum of up to 200 particle jets. The classification task is Lorentz invariant, because a rotated or boosted input momentum should belong to the same category.

In this task, we set the generator to have up to 7 channels, which is slightly more than enough to capture the structure of 6-dimensional  $SO(1, 3)^+$ . We use cosine similarity as between-channel regularization function  $l_{\text{chreg}}$ .

The results are shown in Figure 4. The four dimensions in the matrix correspond to the 4-momentum  $(E/c, p_x, p_y, p_z)$ . LieGAN is successful in recovering the  $SO(1, 3)^+$  group. Its channels 2, 5, 6 correspond to  $SO(3)$  rotation, and channels 0, 1, 3 indicate boost along x-, y- and z-axis. Besides, the generator learns an additional Lie algebra element that scales different input dimensions with approximately the same amounts. This result suggests that LieGAN is capable of discovering high-dimensional Lie groups and also decoupling the group structure to a simple and interpretable representation of Lie algebra basis.

It is also possible to inject this knowledge of Lie group symmetry into existing prediction models. Following the guideline in Section 5.2, we compute the invariant metric of the discovered symmetry (Figure 4), which is almost identical to the true Minkowski metric, with a cosine correlation of  $-0.9975$ . The computed metric is used to construct the LieGNN equivariant to the discovered group. Table 3

shows the prediction results. Without requiring any prior knowledge, LieGNN with the metric derived from LieGAN discovery reaches the performance of LorentzNet (Gong et al., 2022) with the true Minkowski metric.

## 7. Conclusion

In this paper, we present a method of discovering symmetry from training dataset alone with generative adversarial network. Our proposed framework addresses the discovery of various symmetries, including continuous Lie group symmetries and discrete subgroup symmetries, which is a significant step forward compared to existing symmetry discovery methods with relatively narrow search space for symmetry. We also develop pipelines for utilizing the learned symmetry in downstream prediction tasks through equivariant model and data augmentation, which proves to improve prediction performance on a variety of datasets.

This work currently deals with global symmetry of subgroups of general linear groups. However, it is also possible to apply this framework to more general scenario of symmetry discovery, such as non-connected Lie group symmetry, nonlinear symmetry and gauge symmetry, by replacing the simple linear transformation generator in LieGAN with more sophisticated structure. For instance, nonlinear symmetry could possibly be found by adding layers in generator to project the input to a space with linear symmetry.

Moreover, LieGAN shows tremendous potential in its application to supervised prediction tasks, which suggests that automatic symmetry discovery methods may eventually replace the need of human prior knowledge about symmetry. However, this ultimate vision can be fully realized only if equivariant neural network models can be implemented for more general choices of symmetry groups rather than a few specific symmetries. We have demonstrated in this work how to incorporate the discovered symmetry into some equivariant models including EMLP and EGNN, which we hope could inspire further exploration in this topic.



## Acknowledgement

This work was supported in part by the U.S. Department Of Energy, Office of Science, U. S. Army Research Office under Grant W911NF-20-1-0334, Google Faculty Award, Amazon Research Award, and NSF Grants #2134274, #2107256 and #2134178.

## References

- Alet, F., Doblar, D., Zhou, A., Tenenbaum, J., Kawaguchi, K., and Finn, C. Noether networks: meta-learning useful conserved quantities. *Advances in Neural Information Processing Systems*, 34:16384–16397, 2021.
- Antoniou, A., Storkey, A., and Edwards, H. Data augmentation generative adversarial networks. *arXiv preprint arXiv:1711.04340*, 2017.
- Bekkers, E. J. B-spline cnns on lie groups. *arXiv preprint arXiv:1909.12057*, 2019.
- Benton, G., Finzi, M., Izmailov, P., and Wilson, A. G. Learning invariances in neural networks from training data. *Advances in neural information processing systems*, 33:17605–17616, 2020.
- Cohen, T. and Welling, M. Group equivariant convolutional networks. In *International conference on machine learning*, pp. 2990–2999. PMLR, 2016.
- Cohen, T., Weiler, M., Kicanaoglu, B., and Welling, M. Gauge equivariant convolutional networks and the icosahedral cnn. In *International conference on Machine learning*, pp. 1321–1330. PMLR, 2019a.
- Cohen, T. S., Geiger, M., Köhler, J., and Welling, M. Spherical cnns. *arXiv preprint arXiv:1801.10130*, 2018.
- Cohen, T. S., Geiger, M., and Weiler, M. A general theory of equivariant cnns on homogeneous spaces. *Advances in neural information processing systems*, 32, 2019b.
- Dao, T., Gu, A., Ratner, A., Smith, V., De Sa, C., and Ré, C. A kernel theory of modern data augmentation. In *International Conference on Machine Learning*, pp. 1528–1537. PMLR, 2019.
- Dehmamy, N., Walters, R., Liu, Y., Wang, D., and Yu, R. Automatic symmetry discovery with lie algebra convolutional network. *Advances in Neural Information Processing Systems*, 34:2503–2515, 2021.
- Desai, K., Nachman, B., and Thaler, J. Symmetrygan: Symmetry discovery with deep learning. *arXiv preprint arXiv:2112.05722*, 2021.
- Falorsi, L., de Haan, P., Davidson, T. R., and Forré, P. Reparameterizing distributions on lie groups. In *The 22nd International Conference on Artificial Intelligence and Statistics*, pp. 3244–3253. PMLR, 2019.
- Finzi, M., Stanton, S., Izmailov, P., and Wilson, A. G. Generalizing convolutional neural networks for equivariance to lie groups on arbitrary continuous data. In *International Conference on Machine Learning*, pp. 3165–3176. PMLR, 2020.
- Finzi, M., Welling, M., and Wilson, A. G. A practical method for constructing equivariant multilayer perceptrons for arbitrary matrix groups. In *International Conference on Machine Learning*, pp. 3318–3328. PMLR, 2021.
- Gong, S., Meng, Q., Zhang, J., Qu, H., Li, C., Qian, S., Du, W., Ma, Z.-M., and Liu, T.-Y. An efficient lorentz equivariant graph neural network for jet tagging. *Journal of High Energy Physics*, 2022(7), jul 2022. doi: 10.1007/jhep07(2022)030. URL <https://doi.org/10.1007%2Fjhep07%282022%29030>.
- Goodfellow, I., Pouget-Abadie, J., Mirza, M., Xu, B., Warde-Farley, D., Ozair, S., Courville, A., and Bengio, Y. Generative adversarial networks. *Proceedings of the International Conference on Neural Information Processing Systems (NIPS)*, pp. 2672–2680, 2014.
- Greydanus, S., Dzamba, M., and Yosinski, J. Hamiltonian neural networks. *Advances in neural information processing systems*, 32, 2019.
- Kasieczka, G., Plehn, T., Thompson, J., and Russell, M. Top quark tagging reference dataset, March 2019. URL <https://doi.org/10.5281/zenodo.2603256>.
- Kingma, D. P. and Welling, M. Auto-encoding variational bayes. *arXiv preprint arXiv:1312.6114*, 2013.
- Kipf, T. N. and Welling, M. Semi-supervised classification with graph convolutional networks. *arXiv preprint arXiv:1609.02907*, 2016.
- Knapp, A. W. and Knapp, A. W. *Lie groups beyond an introduction*, volume 140. Springer, 1996.
- Kondor, R. and Trivedi, S. On the generalization of equivariance and convolution in neural networks to the action of compact groups. In *International Conference on Machine Learning*, pp. 2747–2755. PMLR, 2018.
- Nowozin, S., Cseke, B., and Tomioka, R. f-gan: Training generative neural samplers using variational divergence minimization. *Advances in neural information processing systems*, 29, 2016.

- Romero, D. W. and Lohit, S. Learning partial equivariances from data. *arXiv preprint arXiv:2110.10211*, 2021.
- Satorras, V. G., Hoogeboom, E., and Welling, M. E (n) equivariant graph neural networks. In *International conference on machine learning*, pp. 9323–9332. PMLR, 2021.
- Wang, R., Walters, R., and Yu, R. Incorporating symmetry into deep dynamics models for improved generalization. In *International Conference on Learning Representations*, 2021. URL [https://openreview.net/forum?id=wta\\_8Hx2KD](https://openreview.net/forum?id=wta_8Hx2KD).
- Wang, R., Walters, R., and Yu, R. Approximately equivariant networks for imperfectly symmetric dynamics. *arXiv preprint arXiv:2201.11969*, 2022.
- Weiler, M. and Cesa, G. General e (2)-equivariant steerable cnns. *Advances in Neural Information Processing Systems*, 32, 2019.
- Worrall, D. and Welling, M. Deep scale-spaces: Equivariance over scale. *Advances in Neural Information Processing Systems*, 32, 2019.
- Zaheer, M., Kottur, S., Ravanbakhsh, S., Poczos, B., Salakhutdinov, R. R., and Smola, A. J. Deep sets. *Advances in neural information processing systems*, 30, 2017.
- Zhou, A., Knowles, T., and Finn, C. Meta-learning symmetries by reparameterization. *arXiv preprint arXiv:2007.02933*, 2020.
- Zhu, J.-Y., Park, T., Isola, P., and Efros, A. A. Unpaired image-to-image translation using cycle-consistent adversarial networks. In *Proceedings of the IEEE international conference on computer vision*, pp. 2223–2232, 2017.

## A. Proofs

### A.1. Optimizing the GAN loss function

We show in this section how optimizing the GAN loss function can lead to proper symmetry discovery. We assume in the first place the existence of a symmetry group and derive the properties of loss when the generator learns this group or its subgroup. We use the definition of perfect symmetry, that is,  $gf(x) = f(gx)$  or  $P_d(gf(x)|gx) = 1$  for symmetry group elements  $g$ . We use  $p_d$  and  $p_{gen}$  to denote original data distribution and generated distribution.

**Assumption 1.** There exists a maximal subgroup of  $GL(n)$ , denoted as  $G^*$ , which  $y = f(x)$  is equivariant to. That is,  $\forall g \in G^*, gy = f(gx); \forall g \in GL(n) \setminus G^*, p_d(gy \neq f(gx)) > 0$ .

**Theorem 1.** The generator can achieve zero JS divergence by learning a maximal subgroup  $G^* \subset GL(n)$  with respect to which  $y = f(x)$  is equivariant if  $p_d(x)$  is distributed proportionally to the volume of inverse group element transformation along each orbit of  $G^*$ -action on  $\mathcal{X}$ , that is,  $p_d(gx_0) \propto |\rho_{\mathcal{X}}(g^{-1})||\rho_{\mathcal{Y}}(g^{-1})|$ .

*Proof.* Revisiting Eq (3), the generated distribution is given by

$$p_{gen}(x, y) = \int_{G^*} \mu(g) p_d(g^{-1}x) p_d(g^{-1}y|g^{-1}x) / |\rho_{\mathcal{X}}(g)| |\rho_{\mathcal{Y}}(g)| dg \quad (12)$$

If  $p_d(x)$  is proportionally distributed along each orbit of  $G^*$ -action on  $\mathcal{X}$ , then

$$p_{gen}(x, y) = \int_{G^*} \mu(g) p_d(x) p_d(g^{-1}y|g^{-1}x) dg \quad (13)$$

For any group element  $g \in G^*$ ,  $p_d(y|x) = p_d(g^{-1}y|g^{-1}x)$ . Therefore,

$$p_{gen}(x, y) = \left( \int_{G^*} \mu(g) dg \right) p_d(x) p_d(y|x) \quad (14)$$

$$= p_d(x, y) \quad (15)$$

As this equality holds for all  $(x, y)$ , we have zero divergence between these two distributions,  $p_d$  and  $p_{gen}$ .  $\square$

While this distribution condition is often not satisfied in practice, we further show that under certain assumptions on data and an ideal discriminator, a nontrivial Lie subgroup of the true symmetry group corresponds to a local minimum of generator loss function.

**Assumption 2.** For each datapoint from the original distribution, transformations outside that maximal subgroup  $G_T$  on it would not produce a valid datapoint. Formally, denoting  $\bar{G}^* = GL(n) \setminus G^*$ ,  $\int_{\bar{G}^*} \mu(g) p_d(gy|gx) dg = 0$ . (While there might be slim chances that  $gf(x) = f(gx)$  for some  $g \in \bar{G}^*$ , the integration can still yield zero as long as we parameterize  $\mu(g)$  with good properties.)

**Assumption 3.** For each orbit  $[x]$  of  $G^*$  with  $P_d([x]) > 0$ ,  $\exists x_0 \in [x], c > 0, m > 0$  s.t.  $\forall g \in \delta_0(m), p_d(gx_0) \geq c, p_d(g^2x_0) \geq c$ , and  $V(g) = |\rho_{\mathcal{X}}(g)||\rho_{\mathcal{Y}}(g)| \in (v_m, V_m)$ , where  $\delta_0(m)$  is a neighborhood of  $\text{id}$  with  $P_\mu(\delta_0(m)) = m$  and  $V_m > v_m > 0$  are constants depending on  $m$ .

This is actually a much more relaxed version of distribution constraint along the group action orbits in Theorem 1, which may be unrealistic. We assume instead that there exists a continuous neighborhood in each orbit where the density of  $x$  is above some threshold.

**Theorem 2.** Under assumptions 1, 2 and 3, the GAN loss function under the ideal discriminator  $L(\Phi, D^*)$  is lower with a generator that learns a subspace of the true Lie algebra  $\mathfrak{g}^*$  than a generator with an orthogonal Lie algebra to  $\mathfrak{g}^*$ . That is, if  $\mathfrak{g}_1 \cap \mathfrak{g}^* \neq \{0\}$ ,  $\mathfrak{g}_2 \cap \mathfrak{g}^* = \{0\}$ , then  $L(\mathfrak{g}_1, D^*) < L(\mathfrak{g}_2, D^*) = 0$ .

*Proof.* As an established result in GAN, the optimal discriminator for the loss function (2) is

$$D^*(x, y) = \frac{p_d(x, y)}{p_d(x, y) + p_{gen}(x, y)} \quad (16)$$

Substituting (16) into (2), we get

$$L(\Phi, D^*) = \int p_d(x, y) \log \frac{p_d(x, y)}{p_d(x, y) + p_{gen}(x, y)} + p_{gen}(x, y) \log \frac{p_{gen}(x, y)}{p_d(x, y) + p_{gen}(x, y)} dx dy \quad (17)$$

$$= \int_{p_d(x, y) \neq 0} p_d(x, y) \log \frac{p_d(x, y)}{p_d(x, y) + p_{gen}(x, y)} + p_{gen}(x, y) \log \frac{p_{gen}(x, y)}{p_d(x, y) + p_{gen}(x, y)} dx dy \quad (18)$$

where, denoting  $\tilde{\mu}(g) = \mu(g)/|\rho_X(g)||\rho_Y(g)|$ ,

$$p_{gen}(x, y) = \int_g \tilde{\mu}(g) p_d(g^{-1}x) p_d(g^{-1}y | g^{-1}x) dg \quad (19)$$

Because the Haar measure  $dg$  is invariant to inversion, we have

$$p_{gen}(x, y) = \int_g \tilde{\mu}(g^{-1}) p_d(gx) p_d(gy | gx) dg \quad (20)$$

In practice, we use Gaussian distribution for  $\mu(g)$ , which assigns the same probability for a group element and its inverse. (This is also true for many other common choices of distribution, such as uniform distribution centered at origin.) Therefore, denoting  $V(g) = |\rho_X(g)||\rho_Y(g)|$ ,

$$p_{gen}(x, y) = \int_g \mu(g) p_d(gx) p_d(gy | gx) |\rho_X(g)||\rho_Y(g)| dg \quad (21)$$

$$= \int_g \mu(g) p_d(gx) p_d(gy | gx) V(g) dg \quad (22)$$

It is easy to show that the Lie group generated by the intersection of two Lie algebras coincides with the intersection of Lie groups generated by these two Lie algebras, respectively. Therefore, as  $\mathfrak{g}_2 \cap \mathfrak{g}_T = \{\mathbf{0}\}$ ,  $G_2 \cap G_T = \{\text{id}\}$ . According to Assumption 2,

$$p_{gen}(x, y; G_2) = \int_g \mu(g) p_d(gx) p_d(gy | gx) V(g) dg \quad (23)$$

$$= \int_{g \in \delta_0(1-\eta)} \mu(g) p_d(gx) p_d(gy | gx) V(g) dg + \int_{g \notin \delta_0(1-\eta)} \mu(g) p_d(gx) p_d(gy | gx) V(g) dg \quad (24)$$

$$\leq \int_{g \in \delta_0(1-\eta)} M \mu(g) p_d(gy | gx) dg + \int_{g \notin \delta_0(1-\eta)} \mu(g) p_d(gx) V(g) dg \quad (25)$$

$$= 0 + \int_{g \notin \delta_0(1-\eta)} \mu(g) p_d(gx) V(g) dg \quad (26)$$

where, following the notations in Assumption 3,  $\delta_0(1-\eta)$  is the neighborhood of  $\text{id}$ ,  $P_\mu(\delta_0(1-\eta)) = 1-\eta$ , and  $V(g) \leq V_{1-\eta}$ . Therefore, there exists an upper bound  $M = \max_{g \in \delta_0(1-\eta)} p_d(gx) V(g)$ .

For the integral on  $g \notin \delta_0(1-\eta)$ , as the Gaussian density  $\mu(g)$  decays exponentially with  $V(g)$  and  $p_d(gx)$  has an upper bound,  $\forall \epsilon > 0, \exists \eta$  s.t.  $\int_{g \notin \delta_0(1-\eta)} \mu(g) p_d(gx) V(g) dg < \epsilon$ .

Therefore,  $p_{gen}(x, y; G_2) = 0$  and  $L(\mathfrak{g}_2, D^*) = 0$ .

On the other hand,  $\mathfrak{g}_1 \cap \mathfrak{g}^* \neq \{\mathbf{0}\} \Rightarrow G_1 \cap G^* \neq \{\text{id}\}$ . We consider the integral (18) along each possible orbit of  $G^*$ . According to Assumption 3, there exists an  $x$ -neighborhood  $X = \delta_0(m)x_0$  s.t.  $\forall x \in X, p_d(x, f(x)) > c$ . For the generated

distribution on this neighborhood, we have

$$p_{gen}(x, f(x)) = \int_g \mu(g) p_d(gx) V(g) dg \quad (27)$$

$$\geq \int_{g \in \delta_0(m)} \mu(g) p_d(gx) V(g) dg \quad (28)$$

$$\geq \int_{g \in \delta_0(m)} \mu(g) cv_m dg \quad (29)$$

$$= mcv_m > 0 \quad (30)$$

As the supports of  $p_d$  and  $p_{gen}$  overlap on this neighborhood, we have  $L(\mathfrak{g}_1, D^*) < 0 = L(\mathfrak{g}_2, D^*)$ .  $\square$

### A.2. Experiment Result on 2-Body Trajectory Dataset

In Figure 2c, we observe an unfamiliar symmetry representation. In fact, this is another possible representation for rotation symmetry. The learned Lie algebra basis  $L$  can be expressed in the following form after discarding the noise:

$$R = \begin{bmatrix} 0 & -1 \\ 1 & 0 \end{bmatrix}$$

$$L = \begin{bmatrix} R & & -R & \\ & R & & -R \\ -R & & R & \\ & -R & & R \end{bmatrix}$$

Computing the matrix exponential gives

$$\exp(\theta L) = \begin{bmatrix} L(\theta) & & -L(\theta) & \\ & L(\theta) & & -L(\theta) \\ -L(\theta) & & L(\theta) & \\ & -L(\theta) & & L(\theta) \end{bmatrix} + I$$

$$L(\theta) = \sum_{k=0}^{+\infty} \frac{2^{2k} (-1)^k \theta^{2k+1}}{(2k+1)!} R + \sum_{k=1}^{+\infty} \frac{2^{2k-1} (-1)^k \theta^{2k}}{(2k)!} I$$

As the origin for this dataset is at the center of mass and  $m_1 = m_2$ , we have  $\mathbf{q}_1 = -\mathbf{q}_2$  and  $\mathbf{p}_1 = -\mathbf{p}_2$ . Therefore,

$$\exp(\theta L) \begin{bmatrix} \mathbf{q}_1 \\ \mathbf{p}_1 \\ \mathbf{q}_2 \\ \mathbf{p}_2 \end{bmatrix} = \text{diag}(I + 2L(\theta)) \begin{bmatrix} \mathbf{q}_1 \\ \mathbf{p}_1 \\ \mathbf{q}_2 \\ \mathbf{p}_2 \end{bmatrix}$$

$$I + 2L(\theta) = \sum_{k=0}^{+\infty} \frac{2^{2k+1} (-1)^k \theta^{2k+1}}{(2k+1)!} R + \sum_{k=0}^{+\infty} \frac{2^{2k} (-1)^k \theta^{2k}}{(2k)!} I$$

$$= \begin{bmatrix} \cos 2\theta & -\sin 2\theta \\ \sin 2\theta & \cos 2\theta \end{bmatrix}$$

which indicates that this is another representation for rotation specific to this dataset.

### A.3. Computing Group Invariant Metric Tensor

**Proposition 1.** Given a Lie algebra basis  $\{L_i \in \mathbb{R}^{k \times k}\}_{i=1}^c$ ,  $\eta(u, v) = u^T J v$  ( $u, v \in \mathbb{R}^k, J \in \mathbb{R}^{k \times k}$ ) is invariant to infinitesimal transformations in the Lie group  $G$  generated by  $\{L_i\}_{i=1}^c$  if and only if  $L_i^T J + J L_i = 0$  for  $i = 1, 2, \dots, c$ .

*Proof.* An infinitesimal transformation in group  $G$  generated by the given Lie algebra basis can be written as the matrix

representation  $g = I + \sum_i \epsilon_i L_i$ .

$$\eta(u, v) = \eta(gu, gv) \quad (31)$$

$$\iff u^T J v = u^T g^T J g v \quad (32)$$

$$\iff u^T (I + \sum_i \epsilon_i L_i^T) J (I + \sum_i \epsilon_i L_i) v = u^T J v \quad (33)$$

$$\iff u^T J v + u^T (\sum_i \epsilon_i (L_i^T J + J L_i)) v + O(\epsilon^2) = u^T J v \quad (34)$$

$$\iff u^T (\sum_i \epsilon_i (L_i^T J + J L_i)) v = 0, \forall u, v \in \mathbb{R}^n \quad (35)$$

As this holds for any infinitesimal transformation  $g$ , we can set  $\epsilon_{-i} = 0$  to get

$$\epsilon_i (L_i^T J + J L_i) = 0, i = 1, 2, \dots, c \quad (36)$$

Therefore,  $L_i^T J + J L_i = 0, i = 1, 2, \dots, c$ .

On the other hand, if  $L_i^T J + J L_i = 0, i = 1, 2, \dots, c$ , then

$$\sum_i \epsilon_i (L_i^T J + J L_i) = 0, \forall \epsilon \in \mathbb{R}^c \quad (37)$$

□

## B. Experiment Details

### B.1. N-Body Trajectory

We use the code from Hamiltonian Neural Networks<sup>1</sup> (Greydanus et al., 2019) to generate the dataset for this task. We construct the train and test sets with different distributions to test the generalization ability of the models. Specifically, we sort the samples in terms of the polar angle of the position of the first particle at the starting timestep of trajectory, and divide the sorted dataset into train and test sets.

The task for this dataset is to predict  $K$  future timesteps of 2-body movement based on  $P$  past timesteps of observation, where the feature for each timestep has 8 dimensions, consisting of the positions and momentums of two bodies:  $[q_{1x}, q_{1y}, p_{1x}, p_{1y}, q_{2x}, q_{2y}, p_{2x}, p_{2y}]$ . In our experiment, we set  $P = K = 5$ . When discovering symmetry, the LieGAN generator takes both the past observations and future predictions as input, yielding an input dimension of 80. The generator transforms each timestep at the same time, which means that it is learning a group representation of  $\mathbb{R}^{8 \times 8}$  that acts simultaneously on each of the past input and future output timesteps. On the other hand, we use a 3-layer MLP as with discriminator, with input dimension 80, hidden dimension 512, and leaky ReLU activation with negative slope 0.2. We use only the regularization against identical transformations, i.e.  $l_{\text{reg}}(x, y)$  in (5), with the regularization coefficient  $\lambda = 1$ . but not the between-channel regularization in (6), because the generator only has a single channel and there is no need for it. The learning rates for the discriminator and the generator are set to 0.0002 and 0.001, respectively. LieGAN is trained adversarially for 100 epochs.

We also experiment with more settings than 2-body movement. Concretely, We increase the number of moving bodies to 3, which leads to more complicated 3-body movement. Despite the increased complexity, LieGAN is still able to discover the rotation symmetry in this case, as is shown in Figure 5.

In the prediction task with equivariant model, we use EMLP with 3 hidden layers and a hidden representation of  $5V$ , where  $V$  stands for an 8-dimensional vector just as the feature for each timestep. We train all EMLPs constructed with different equivariances with  $\text{lr}=0.0001$  for 5000 epochs.

As is mentioned in Section 5.2, we slightly modified the EMLP implementation to adapt to the noised discovery result from LieGAN. EMLP projects the network weight to an equivariant subspace, which is the null space of the constraint matrix derived from the provided equivariance and input and output representations. The null space is computed with

<sup>1</sup><https://github.com/greydanus/hamiltonian-nn>

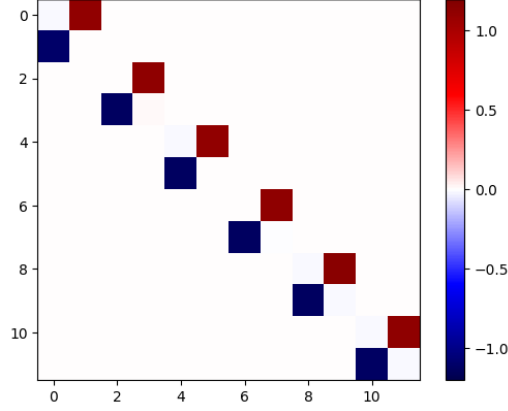


Figure 5. Symmetry discovery result on 3-body trajectory prediction dataset. LieGAN can also learn an accurate representation of rotation symmetry as in the case of 2-body dataset.

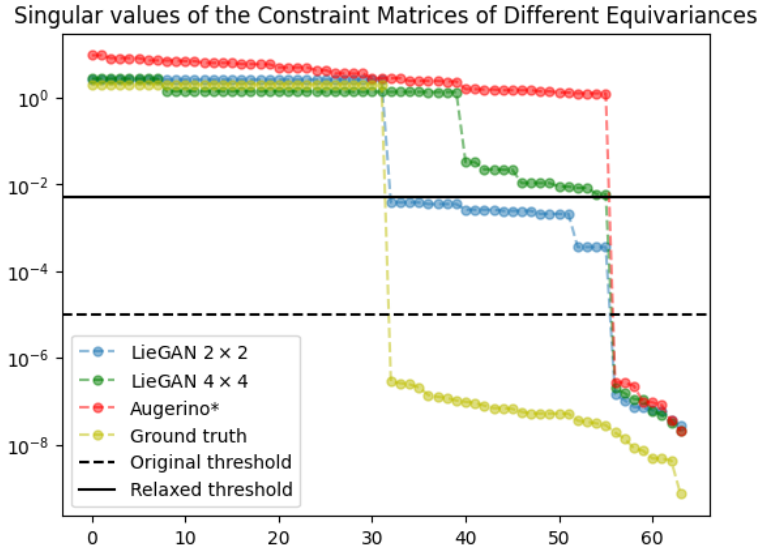


Figure 6. Singular values of the EMLP constraint matrices derived from different equivariances under the representation of group actions on weight matrices mapping from  $V_1 \rightarrow V_2$ , where  $V_1$  and  $V_2$  are both 8-dimensional vector spaces. The  $y$  axis is log-scaled for better visualization. It can be observed that the singular values of the constraint matrix corresponding to the symmetry discovered by LieGAN have a sharp decrease at the same position as the matrix for ground truth symmetry. This suggests that we can slightly relax the singular value threshold to obtain a higher dimensional equivariant subspace.



SVD. This method usually works for common handpicked symmetries, such as Euclidean group and Lorentz group, which typically have sparse and clean matrix representations. However, the symmetry discovered by LieGAN inevitably has some numerical error. While such error could be largely negligible when we visualize the discovered symmetry or use it for data augmentation, it will cause problem in the SVD procedure in the EMLP implementation. Even a small noise that changes a matrix representation entry from zero to small nonzero values could result in a constraint matrix with higher rank, which then leads to a lower dimensional equivariant subspace and a lower rank weight matrix. However, we can raise the singular value threshold to larger values to calculate an approximate null space, which has higher dimensions. Figure 6 shows how we modify the singular value threshold. The original EMLP implementation sets a threshold of  $1e-5$ . With this threshold, the symmetries discovered by LieGAN lead to a weight matrix that maps each input vector to each hidden vector with a rank of 8, significantly lower than 32, which is the case for ground truth rotation symmetry. However, it can also be observed that the singular values of the constraint matrix corresponding to LieGAN symmetry have a sudden fall at the same position as the matrix for ground truth symmetry. Therefore, we can raise the singular value threshold to  $5e-3$ , which is still reasonably small, and obtain a 32-dimensional approximately equivariant subspace for the discovered symmetry. This procedure proves to significantly improve prediction performance for EMLP constructed with the discovered symmetry.

## B.2. Synthetic Regression

This is a regression problem given by  $f(x, y, z) = z / (1 + \arctan \frac{y}{x} \bmod \frac{2\pi}{k})$ . This function is invariant to rotations of a multiple of  $2\pi/k$  in  $xy$  plane, which form a discrete cyclic subgroup of  $SO(2)$  with a size of  $k$ . In our experiment, we construct the dataset with  $k = 7$ . We randomly sample 20000 inputs  $(x, y, z)$  from a standard multivariate Gaussian distribution and calculates the output analytically. For symmetry discovery, we use a generator with a single channel of  $\mathbb{R}^{3 \times 3}$  matrix representation and a 3-layer MLP discriminator with input dimension 4 (which is  $(x, y, z, f)$ ), hidden dimension 512, and leaky ReLU activation with negative slope 0.2. The coefficient distribution in the generator is set to a uniform distribution on integer grid between  $[-10, 10]$ . We use regularization term  $l_{\text{reg}}$  with coefficient  $\lambda = 0.01$ . The learning rates for the discriminator and the generator are set to 0.0002 and 0.001, respectively. LieGAN is trained for 100 epochs.

## B.3. Top Quark Tagging

For symmetry discovery, we use a generator with 7 channels of  $\mathbb{R}^{4 \times 4}$  matrix representations acting on the input 4-momenta  $(E/c, p_x, p_y, p_z)$ . The input consists of the momenta of up to 200 constituents for each sample, sorted by the transverse momentum of each constituents. We truncate the input to the momenta of the two leading constituents, which gives an input dimension of 8. As this classification task is invariant, the generator does not change the category label associated with each sample. The discriminator takes both the transformed input momenta  $gx$  and the output label  $gy = y$  as its input. It first transforms  $y$  to a real-valued vector with an embedding layer, and then concatenates the embedding with  $gx$ , and passes them through a 3-layer MLP with hidden dimension 512 and leaky ReLU activation with negative slope 0.2. We use regularizations  $l_{\text{reg}}$  with coefficient  $\lambda = 1$  and  $l_{\text{chreg}}$  with coefficient  $\eta = 0.1$ . The learning rates for the discriminator and the generator are set to 0.0002 and 0.001, respectively. LieGAN is trained for 100 epochs.

For prediction with LieGNN, we first calculate the invariant metric tensor based on the discovered symmetry according to Equation (10). We optimize the objective with  $a = 0.0005$  and matrix max norm using a gradient descent optimizer with step size of  $1 \times 10^{-5}$ . Then, we build the LieGNN prediction model based on LorentzNet implementation<sup>2</sup>. The model has 6 group equivariant blocks with 72 hidden dimensions. We use a dropout rate of 0.2 and weight decay rate of 0.01. The model is trained for 35 epochs with a learning rate of 0.0003. These settings are the same for LorentzNet and LieGNN.

<sup>2</sup><https://github.com/sdogsq/LorentzNet-release>